BOLLETTINO DI GEOFISICA TEORICA ED APPLICATA VOL. 40, N. 3-4, pp. 277-283; SEP.-DEC. 1999

New simulations for the spaceborne gravimetry inversion

A. ALBERTELLA, F. MIGLIACCIO and F. SANSÒ

Dip. IIAR, Sez. Rilevamento, Politecnico di Milano, Italy

(Received October 5, 1998; accepted August 5, 1999)

Abstract. After a call for proposals from the Italian Space Agency (ASI), for small satellite missions a group of Italian research teams and industries, led by the Politecnico di Milano conceived SAGE. This mission aims at determining the gravity field of the Earth by means of high-low SST, in other words the satellite orbit is determined by GPS, while the non-gravitational perturbations are determined by a three-axes accelerometer. This is basically the same concept of the CHAMP mission (Reigber et al., 1996). SAGE underwent a Phase A Study during the year 1998 (ASI, 1998). In this framework, the task of the Politecnico di Milano group was to analyze the data by means of the spacewise approach. Besides studying new simulations of the data expected from SAGE, the complete spacewise approach requires the inversion of Hill's equations to be performed, to form average values on a regular grid over the sphere and to recover the gravity field coefficients. The simulations are required in order to: assess the accuracy of the data obtained after the inversion of Hill's equations, introducing a realistic measurement noise; formulate the overdetermined boundary value problem to be solved; determine indices enabling the evaluation of the performances of the solution.

1. The concept of space accelerometry

The proposal for the SAGE (Satellite Accelerometry by Gravity Field Exploration) mission consisted in using a GPS receiver together with an accelerometer on a low, polar orbit satellite. The accelerometer proofmass, positioned in the centre of mass of the satellite, is subject to a purely gravitational acceleration g, while the centre of mass of the satellite is subject (besides the same acceleration $\underline{g}$) also to all non-gravitational forces which act on the surface, whose sum is $\underline{f}$. Therefore the accelerometer gives a direct measure of $\underline{f}$.

The GPS tracking (aided by an SLR device) allows the reconstruction (with very high relative

Corresponding author: A. Albertella; Politecnico di Milano - DIIAR, Piazza Leonardo da Vinci 32, Milano, Italy; phone: +39 02 23996509; fax: +39 02 23996530; e-mail: alberta@ipmtf4. topo.polinci.it

precision between two points along an orbit arc) of the satellite trajectory $\underline{x}(t)$. The difference between the "observed" orbit $\underline{x}(t)$ and the orbit $\underline{\tilde{x}}(t)$ modelled by all available information is due to the residual gravitational effects:

$$\underline{\xi}(t) = \underline{x}(t) - \underline{\tilde{x}}(t), \tag{1}$$

where $\underline{\xi}(t)$ is the orbit anomaly, equivalent to a "virtual" orbit ruled by the residual gravitational potential. From $\underline{\xi}(t)$ it is possible, by differentiating and smoothing, to obtain observed values of $\underline{g}$ along the orbit, which can be integrated to give the harmonic coefficients of the field, in the framework of an overdetermined boundary value problem.

In particular, we write the equation of the motion of the satellite as (Bassanino et al., 1992)

$$\ddot{\underline{x}} = \nabla u_o(\underline{x}) + \nabla \delta u(\underline{x}) + \underline{f}_g(\underline{x}) + \underline{f}_{ng}(\underline{x}), \tag{2}$$

considering the gravitational potential $u(x)$ as the sum of a reference potential $u_0(x)$ and a residual part $\delta u(\underline{x})$. In this eq., $\underline{f}_g(\underline{x})$ represents the effects of the sun, moon and tides (which can be modelled) and $\underline{f}_{ng}(\underline{x})$ represents the effect of the surface forces (mainly due to the drag, which is measured by the accelerometer). It must be remarked that $\underline{f}_g$ and $\underline{f}_{ng}$ can be computed along the nominal orbit without significant errors.

The residual gravitational effects $\delta\underline{g}$ along the orbit can be obtained by inverting Hill's eqs., which are written here under the hypotheses that $\underline{\xi}$ is small and that the orbit arc is circular:

$$\begin{aligned} \ddot{\xi}_a + 2\omega\dot{\xi}_r &= \delta g_a \\ \ddot{\xi}_r + 2\omega\dot{\xi}_a - 3\omega^2\xi_r &= \delta g_r \\ \ddot{\xi}_o + \omega^2\xi_o &= \delta g_o . \end{aligned} \tag{3}$$

The indices *a,r,o* respectively denote the along-track, radial and orthogonal (out of plane) component.

This system is inadequate to produce realistic orbit ephemerides; nevertheless, it is useful because it can certainly be used to produce simulations, to understand how well (3) can be inverted. The general solution of Eq. (3) can be written as,

$$\underline{\xi}(t) = \underline{\xi}_h(t) + \underline{\xi}_P(t), \tag{4}$$

$$\begin{cases} \xi_{ha} = D - 3At - 2B\sin nt + 2C\cos nt \\ \xi_{hr} = \dfrac{2A}{r} B\cos nt + C\sin nt \\ \xi_{ho} = F\sin nt + E\cos nt, \end{cases} \tag{5}$$

$$\begin{cases} \xi_{pa} = -\dfrac{2}{n}\displaystyle\int_0^t [1-\cos n(t-\tau)]\delta g_r(\tau)d\tau + \dfrac{4}{n}\int_0^t \sin n(t-\tau)\delta g_a(\tau)d\tau - 3\int_0^t (t-\tau)\delta g_r(\tau)d\tau \\ \xi_{pr} = \dfrac{1}{n}\displaystyle\int_0^t \sin n(t-\tau)\delta g_r(\tau)d\tau + \dfrac{2}{n}\int_0^t [1-\cos n(t-\tau)]\delta g_a(\tau)d\tau \\ \xi_{po} = \dfrac{1}{n}\displaystyle\int_0^t \sin n(t-\tau)\delta g_o(\tau)d\tau. \end{cases} \tag{6}$$

So what we have to do is basically to invert Eqs. (4), (5), (6) for δg_a, δg_r, δg_o.

This can be done by a spacewise approach, which amounts to inverting Eqs. (4), (5), (6) directly with a suitable stochastic inverse method; this step provides the vector (δg_a, δg_r, δg_o) on a sphere at satellite altitude; the vector is then used to estimate the coefficients T_{lm} via integration with spherical harmonics.

2. Numerical tests with the spacewise approach

In order to verify the theoretical procedure described in Section 1, it was decided to produce simulated data to be treated in the spacewise approach. Using the EGM96 gravity model, the three components of the residual gravity accelerations were computed at points spanning a quarter of an orbit[1], with the initial condition that latitude $\varphi = 0$ when $t = 0$ both for ascending and for descending arcs. Other parameters of the simulation can be found in Table 1. The interval between two subsequent points along the arc is $\Delta t = 5$ *s*.

To obtain the orbit anomalies according to Eq. (3), only the particular solution was used, in fact the homogeneous part of the integral is irrelevant to our reasoning. This happens because in the subsequent estimation procedure of δg (obtained by applying the Hill operator) the contribution of the homogeneous solution Eq. (5) is equal to zero.

[1]One choice is fundamental, namely to use a short arc approach, inverting half a cycle at a time so that the central point of the arc has a maximum distance from the ends equal to a quarter of a cycle. First of all this approach shows that data could be treated even in case of (relatively) frequent interruptions without degrading the mission. Moreover this choice is done to be sure that the noise in $\xi(t)$ is limited to 1÷2 cm.

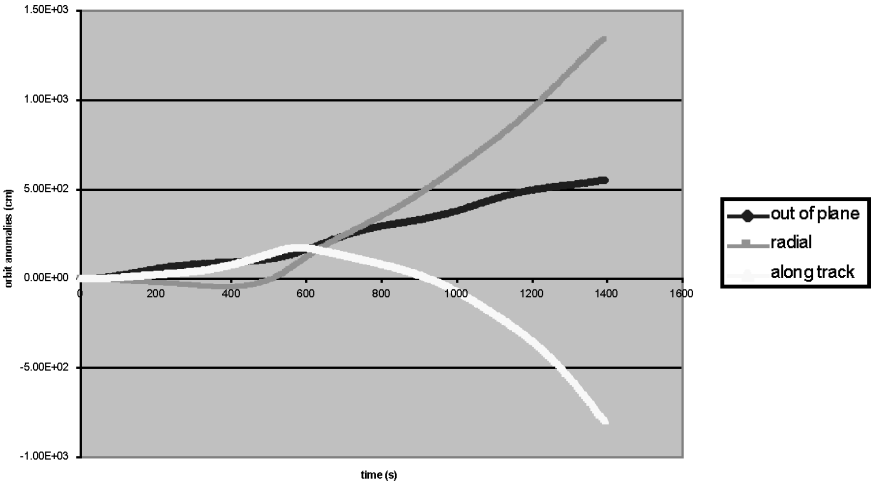

Fig. 1 - An example of simulated orbit anomalies along a generic arc.

By using a simple numerical integration algorithm, the three components ξ_{pa} , ξ_{pr} , ξ_{po} were computed.

Afterwards, from the data as represented in Fig. 1, two contributions were subtracted: one represents the average value of the data themselves, while the other is the trend produced by the homogeneous solution of Eq. (3). Before applying the estimation procedure, a white noise with mean square value equal to 2 cm was added to the "observations" (cfr. Fig. 2).

Starting from the simulated observations $\underline{\xi}$, we now had to study the behaviour of the estimated values of $\delta\underline{g}$ over a regular grid, covering the Earth's surface. In order to do this, we decided to choose a sample area with dimensions 2°×2°: over this area, data were simulated (according to the previously described procedure) for a mission lifetime of one year, corresponding to 15 ascending and 15 descending arcs.

The idea was to derive the signal $\delta\underline{g}$ from $\underline{\xi}$ and observation equations Eq. (3) by applying a collocation approach along the arc.

To optimize the collocation procedure, the empirical covariance function was estimated after grouping the arcs in sets of five each and referring the averaged data (five by five) to the points of the medium arc. However, the collocation estimate of the functionals, needed to invert Hill's equations, was subsequently performed at the original points of each arc.

Table 1 - Parameters used for the simulation of data to be treated in the spacewise approach.

l_{min}	11
l_{max}	90
R (cm)	637813630
GM (cm^3/s^2)	$3986004.415\ 10^{14}$
W (rad/s)	$7292115\ 10^{-11}$
r (cm)	680813630
I	87°

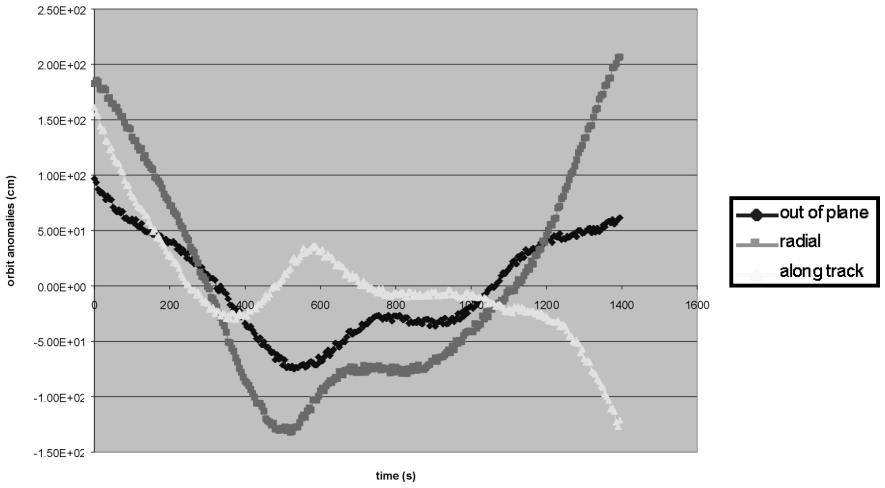

Fig. 2 - Simulated observations, after detrending and adding a white noise with mean square value equal to 2 cm.

The inversion of Hill's equations gave the values of the components $\delta\hat{g}_a$, $\delta\hat{g}_r$, $\delta\hat{g}_o$, at all the observation points of the sample block: by simply averaging the single components, the mean values were obtained. These values, after undergoing a suitable rotation to an Earth-fixed reference system (and assuming no attitude error), were referred to the center point of the block: we call them $\delta\overline{\hat{g}}_\vartheta$, $\delta\overline{\hat{g}}_\lambda$, $\delta\overline{\hat{g}}_r$. The same quantities were also directly simulated using the EGM96 gravity model:

$$\delta g_r = \frac{\partial T}{\partial r}$$

$$\delta g_\vartheta = \frac{1}{r}\frac{\partial T}{\partial \vartheta} \tag{7}$$

$$\delta g_\lambda = \frac{1}{r\sin\vartheta}\frac{\partial T}{\partial \lambda}$$

where:

$$\frac{\partial T}{\partial r} = -\frac{GM}{R}\frac{1}{r}\left\{\sum_{lm}\left(\frac{R}{r}\right)^{l+1}(l+1)[T_{l,m}\cos m\lambda + T_{l,-m}\sin m\lambda]P_{lm}(\cos\vartheta)\right\}$$

$$\frac{\partial T}{\partial \vartheta} = \frac{GM}{R}\left\{\sum_{lm}\left(\frac{R}{r}\right)^{l+1}[T_{l,m}\cos m\lambda + T_{l,-m}\sin m\lambda]\frac{\partial}{\partial\vartheta}P_{lm}(\cos\vartheta)\right\} \tag{8}$$

$$\frac{\partial T}{\partial \lambda} = \frac{GM}{R}\left\{\sum_{lm}\left(\frac{R}{r}\right)^{l+1}m[T_{l,-m}\cos m\lambda - T_{l,m}\sin m\lambda]P_{lm}(\cos\vartheta)\right\}$$

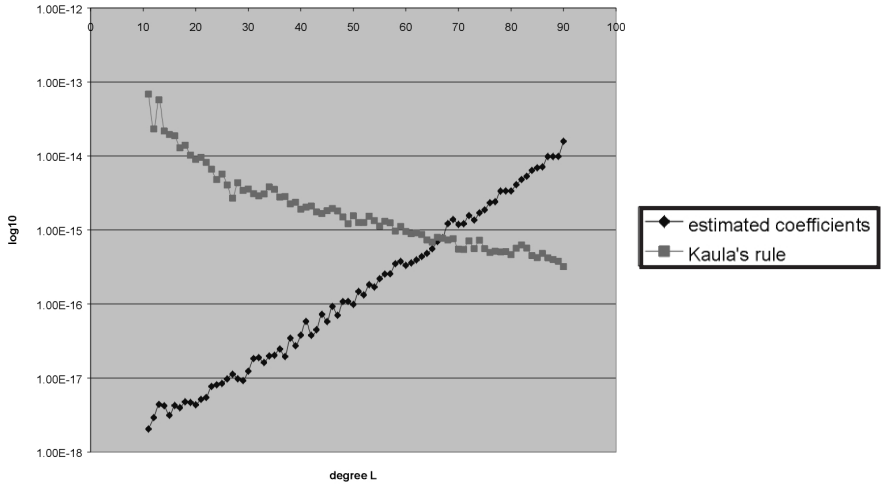

Fig. 3 - Signal-to-noise ratio and maximum estimable degree.

The results of the estimation procedure are summarized in Table 2.

These results quantify the noise produced for each component by the applied collocation procedure. Therefore, three sets of noise data were synthetized, with mean square values equal to those computed from the differences between simulated and estimated values.

3. Recovery of the gravity field coefficients

The final step consisted in computing two sets of harmonic coefficients by discretizing the harmonic analysis formulas for the radial and horizontal components of the gravity field

$$T_{lm}^{1} = -\left(\frac{r}{R}\right)^{l+2} \frac{1}{\frac{\mu}{R^2}(l+1)} \frac{1}{4\pi} \int \left(\frac{\partial T}{\partial r}\right) Y_{lm}(\sigma) d\sigma$$

$$T_{lm}^{2} = \left(\frac{r}{R}\right)^{l+2} \frac{1}{\frac{\mu}{R^2} l(l+1)} \frac{1}{4\pi} \int \nabla_{\sigma}(T Y_{lm}(\sigma)) d\sigma, \tag{9}$$

Table 2 - Comparison between estimated and simulated values.

DIFFERENCES	$\delta\bar{g}_{\vartheta} - \delta\bar{\hat{g}}_{\vartheta}$	$\delta\bar{g}_{\lambda} - \delta\bar{\hat{g}}_{\lambda}$	$\delta\bar{g}_{r} - \delta\bar{\hat{g}}_{r}$
Mean value (mGal)	-0.049	0.066	-0.204
Mean square value (mGal)	0.589	0.317	0.470

which afterwards allowed us to derive the unique weighted estimate represented by

$$\bar{T}_{lm} = \frac{\frac{1}{\sigma_{1l}^2} T_{lm}^1 + \frac{1}{\sigma_{2l}^2} T_{lm}^2}{\frac{1}{\sigma_{1l}^2} + \frac{1}{\sigma_{2l}^2}}, \tag{10}$$

where

$$\sigma_{1l}^2 = \sigma^2(T_{lm}^1) = \left(\frac{r}{R}\right)^{2l+4} \frac{\sigma_r^2}{4\pi\left(\frac{\mu}{R^2}\right)^2 (l+1)^2}$$
$$\sigma_{1l}^2 = \sigma^2(T_{lm}^2) = \left(\frac{r}{R}\right)^{2l+4} \frac{\sigma_h^2}{4\pi\left(\frac{\mu}{R^2}\right)^2 l(l+1)} \tag{11}$$

σ^2_r, σ^2_h being the Wiener variance densities of radial and horizontal components.

An index showing the highest estimable degree is the signal-to-noise ratio, obtained by comparison of the curve of the degree variances given by Kaula's rule with the curve of the degree variances of the estimated model. This gives a maximum attainable degree equal to l_{max} = 49, as shown in Fig. 3.

We took this result as provisory, probably due to a too rough approximation in quadrature formulas. We say this, because a theoretical prediction of l_{max} from a uniform noise of 0.5 mGal resulted in $l_{max} \cong 62$, which by the way is in agreement with the results obtained by the research team working with SAGE simulated data, in the framework of the timewise approach (ASI, 1998).

References

ASI; 1998: *SAGE Phase A Final Report*. Agenzia Spaziale Italiana, 1998.

Bassanino M., Migliaccio F. and Sacerdote F.; 1992: *A BVP approach to the reduction of GPS and accelerometric observations*. In: Colombo O. L. (ed), Proc. Symp. IAG 110 From Mars to Greenland: charting gravity with space and airborne instruments, Springer-Verlag, New York.

ESA; 1998: *European Views on Dedicated Gravity Field Missions: GRACE and GOCE ESD-MAG-REP-CON-001*. ESA, May 1998.

Reigber Ch., Bock R., Forste Ch., Grunwaldt L., Jakowski N., Luhr H., Schwintzer P. and Tilgner C.; 1996: *CHAMP Phase B Executive Summary*. GFZ, STR96/13.